Tropospheric circulation sensitivity to an interactive stratospheric ozone

S. Brand,[1] K. Dethloff,[1] and D. Handorf[1]

S. Brand, K. Dethloff, and D. Handorf, Foundation Alfred Wegener Institute for Polar and Marine Research, Research Unit Potsdam, Telegrafenberg A43, D-14473 Potsdam, Germany. (Sascha.Brand@awi.de, Klaus.Dethloff@awi.de, Doerthe.Handorf@awi.de)

[1]Foundation Alfred Wegener Institute for Polar and Marine Research, Research Unit Potsdam, Potsdam, Germany.

For this conceptual study we focus on the impact of interactive stratospheric ozone chemistry on the tropospheric circulation, using the atmosphere-ocean-sea ice general circulation model (AOGCM) ECHO-GiSP with simplified stratospheric chemistry. The model covers the troposphere and middle atmosphere up to 80 km height. Our results show a clear sensitivity of the tropospheric circulation dynamics to the stratospheric chemistry. With enabled interactive stratospheric chemistry the model tends to the negative phase of the Arctic Oscillation (AO) mode. This also includes an enhanced midlatitudinal planetary and synoptic scale wave activity. The strenghtening of the synoptic scale waves leads to stronger stormtracks, while the planetary scale waves show larger changes outside this particular latitudes. Another tropospheric region, which is influenced by interactive stratospheric chemistry effects, is the tropical troposphere. Due to changes in lower stratospheric ozone concentrations a significant cooling appears in the positive AO-phase compared to the negative phase.

1. Introduction

A current development in coupled climate modeling is to integrate more and more model components in order to detect and to discuss possibly relevant feedback loops between them. Thus, beside the main components atmosphere and ocean, the influences of e.g. atmospheric chemistry, carbon cycles, land use, sea ice, soil and other climate factors are under examination. In this conceptual study we focus on stratospheric ozone chemistry, since some of the most important chemical species such as O_3, CO_2, CH_4 or N_2O are also controlling the middle atmospheric circulation. This is due to the differential warming by absorption of incoming solar ultraviolet- and outgoing terrestrial infrared radiation by these greenhouse gases. However, since there is increasing evidence for a strato-tropospheric dynamical coupling [e.g. *Holton et al.*, 1995; *Song and Robinson*, 2004; *Scaife et al.*, 2005], changes in stratospheric greenhouse gas concentrations and -distributions are likely also to exert a relevant impact on the tropospheric circulation. In turn, the stratospheric chemistry is affected by changes of the stratospheric dynamics, where the intense temperature dependency is most important. But also the accumulation of trace gases is generally altered by the meridional mean circulation, which is connected with the wave forcing by ascending tropospheric planetary waves [*Eichelberger and Hartmann*, 2005]. Because of such complex dependencies the explicit consideration of the interactive coupling between stratospheric chemistry and -dynamics appears to be a crucial issue. As a comprehensive model for such a purpose we used the AOGCM ECHO-GiSP with simplified stratospheric chemistry. In this paper we discuss differences between

the results of two 150 year runs, as well as the internal variability in one of these runs, focusing on the troposphere.

2. Model and Experiments

ECHO-GiSP ($\underline{ECHO-G}$ with $\underline{I}$ntegrated $\underline{S}$tratospheric chemistry by AWI Research Unit $\underline{P}$otsdam) is an extension of the coupled AOGCM ECHO-G [*Legutke and Voss*, 1999], where a chemistry part based on the MECCA chemistry module [see *Sander et al.*, 2005] was added. The model includes the 39-level middle atmosphere version [e.g. *Manzini and McFarlane*, 1998] of the atmosphere model ECHAM4 [*Roeckner et al.*, 1996] with a model top at 1 Pa (80 km). It was applied at a spectral resolution of T30. As ocean component the ocean-sea ice model HOPE-G [*Wolff et al.*, 1997] is utilised, using a horizontal resolution of T42 with a refinement towards the equator, and a vertical resolution of 21 levels. For heat and freshwater exchange between the atmosphere- and the ocean component a flux correction is applied.

The chemistry scheme, added to the ECHAM-part of ECHO-GiSP, allows gas phase reactions, photolysis reactions and heterogenous reactions on polar stratospheric clouds. In particular we used a setup with 39 chemical species, for which 116 chemical reactions are defined. The species include the main members of the O_x, NO_x, ClO_x, HO_x and BrO_x chemical families, as well as gases like CO, CO_2, CH_4, N_2, H_2, H_2O. All species are transported via the semi-Lagrangian transport scheme by *Rasch and Williamson* [1990]. Furthermore, since our main focus was on impacts of stratospheric chemistry, data from the KASIMA chemistry transport model [*Kouker et al.*, 1999] have been used to provide boundary conditions for the chemical fields in the troposphere. This allows interactive

chemistry and dynamical feedbacks in the stratosphere, while keeping prescribed chemistry in the troposphere in order to avoid a too complex chemistry scheme. Moreover, thereby is no need explicitly to prescribe realistic surface sources and sinks for the chemical species used, which would introduce additional uncertainties.

An important advantage of the simplified stratospheric chemistry within ECHO-GiSP is, that this enabled us to perform two fully coupled long term simulations of 150 simulation years each. Both of them are timeslice experiments under fixed present-day conditions, differing only in the trace gas concentrations used in the ECHO-G radiation scheme [*Morcrette*, 1991]. The so called coupled run, hereafter denoted as COUP, was performed with the interactive chemistry-dynamics coupling, i.e. the radiation scheme was driven by the simulated chemical fields in the stratosphere. For the reference run (REF) climatological trace gas fields were used instead. Since therefore the dynamical variables were not influenced by the modeled chemical constituents in this run, they are equivalent to the ones simulated by the EGMAM-model of the meteorological institute at the FU Berlin. A validation for this model was done by *Huebener et al.* [2007], concluding that the present-day climate is realistically simulated. For both of our simulations (COUP and REF) we chose a spin-up time of 30 years.

3. Simulated Tropospheric Response to Interactive Stratospheric Chemistry

As an indicator for the tropospheric variability, respectively its changes due to the interactive stratospheric chemistry in COUP compared to REF, we first discuss the geopotential height at the 500-hPa pressure level (z_{500}). Thereby in this study we focus on the

northern hemisphere winter period (DJF) as the dynamically most active season, showing 120-year means for the model years 31 to 150.

In figure 1a the z_{500}-differences between COUP and REF are presented. The spatial pattern shows an inverse Arctic Oscillation (AO, introduced by *Thompson and Wallace* [1998]) like behaviour with significant (95% confidence level) negative northern Pacific, positive polar and negative northern Atlantic deviations. Thus, COUP tends to a negative AO phase with a weaker Icelandic low and Azoric high, which is also related to a more negative phase of the North Atlantic Oscillation (NAO, *Hurrell* [1995]). Furthermore the tendency towards the negative AO phase in the troposphere is connected with a warmer, more disturbed stratospheric vortex for COUP compared to a colder and stronger polar vortex for REF (not shown here).

Changes in the atmospheric variability mode of the AO also imply changes in the planetary and synoptic scale wave activity. This is confirmed by figure 1b, where results of a discrete Fourier transform (DFT) for the northern hemisphere lowpass (LP, 10 to 90 d) and bandpass (BP, 2 to 6 d) filtered z_{500}-data are displayed. The mean power (logarithm of squared waveamplitude) for the wavenumbers 1 to 3 (with LP data) generally shows an increase in COUP relative to REF, but with local maxima around $45°N$ and $65°N$ and a minimum near $55°N$. In opposition to this the mean power for the synoptic scale wavenumbers 4 to 10 (with BP data) has only one broad maximum (increase of wave activity) between $50°N$ and $60°N$. Hence, locally the strenghtening of the midlatitudinal stormtracks is anticorrelated to the planetary wave activity. Globally, however, COUP appears with enhanced tropospheric wave activity compared to REF.

For both simulations a principal component analysis (PCA) was carried out to study spatio-temporal variations, using the unfiltered 120-year z_{500}-data sets. Here we show the first PC (PC1), belonging to the leading mode of variability (EOF1), and the associated wavelet transform spectrum [*Torrence and Compo*, 1998] for COUP (figure 2). The spatial pattern of EOF1 (not shown) is close to the AO-like difference pattern COUP-REF in figure 1a. This is consistent with the AO definition of *Baldwin and Dunkerton* [1999] who determined the AO using EOF1 of a composite of normalized geopotential height anomalies from pressure levels between 1000 and 10 hPa. The temporal structure of PC1 (figure 2a) exhibits a clear annual to interannual and decadal scale variability of EOF1. More pronounced this shows up in the wavelet transform spectrum (figure 2b), although at the longer time scales the signal detection is restricted due to the limited length of the time series.

Interpreting PC1 as the modeled time series of the AO, two periods of 8 simulation years each for COUP (see figure 2a) and REF were chosen, representing the positive (AO+) and the negative phase (AO−) of the AO. The mean differences between both AO phases, as shown in figure 3 for the zonal means of the zonal wind u, the temperature T and the ozone concentration O_3, provide further information about the internal varibility within COUP. Within REF (not shown here) there are similar difference patterns for u, T and O_3, with the exception that there is no signal for the tropical temperatures.

For COUP the zonal winds north of about $40°N$ in figure 3a show enhanced values for AO+ compared to AO− in the troposphere and stratosphere up to 1 hPa. Such a positive coupling between the tropospheric AO and the stratospheric polar vortex was also

detected in previous studies as e.g. by *Polvani and Kushner* [2002] or *Norton* [2003]. In the upper troposphere and lower stratosphere negative values of the zonal wind differences (also figure 3a) hint on a weakening of the modeled subtropical jets under AO+ conditions. The tropospheric temperature differences (figure 3b) show negative values of 0.5 to 1 K in the tropics. This cooling effect for AO+ compared to AO− is significant on a confidence level of 95%. Above the tropical cooling there is a lower stratosphere warming of up to 1 to 2 K. Finally (figure 3c) the lower stratospheric differences of the zonal mean ozone concentrations indicate more ozone in the tropics and less ozone towards the higher latitudes for AO+. This ozone difference pattern between the AO phases is likely due to a reduced meridional exchange of air masses as a response to the stronger polar stratospheric vortex in this phase of the AO.

4. Discussion and Conclusions

In this paper it has been shown that the consideration of an interactive stratospheric chemistry scheme can be substantial for climate sensitivity studies even if it is used in a rather simplified way. In particular our results indicate that the tropospheric circulation is clearly affected by the way how the stratospheric ozone chemistry is treated within the model simulations. Among others we detected changes in the DJF z_{500}-field, resembling the structure of the Arctic Oscillation (AO) mode of the tropospheric variability. Thereby the run with enabled interactive stratospheric chemistry (COUP) is shifted towards the negative AO phase compared to the run neglecting this feedback (REF). Additionally we found modifications of the tropospheric planetary and synoptic scale wave activity between our simulations, which generally show enhanced midlatitudinal values for COUP.

This enhancement is consistent with the preference of the more disturbed AO− phase in COUP, but overlayed by a locally anticorrelated behaviour of the two wave types. A possible reason for this anticorrelation, though still speculative at our degree of knowledge demonstrated within this paper, might be due to a quasi-stationary behaviour of the potentially available wave energy on shorter timescales (up to months). On longer timescales (between seasons or from year to year, simulation to simulation) the available wave energy mainly changes with the mid- to highlatitude temperature gradient, allowing systematic setoffs in stormtrack and planetary wave activity. We plan to adress this issue of wave dynamics and interactions in a forthcoming paper.

From previous studies as *Scaife et al.* [2005] it is already known that at least in mid- and high latitudes there is a dependency of tropospheric circulation and surface climate on the stratospheric variability. In agreement with the conclusions of e.g. *Shindell et al.* [2001] and *Stenchikov et al.* [2002] this implies a most likely positive feedback loop between the stratospheric polar vortex, the tropospheric midlatitudinal zonal mean flow, the associated planetary wave activity and their effect back on the stratospheric polar vortex as a possible coupling mechanism. The tropospheric shift to a negative AO phase in COUP could therefore be due to the stratospheric stabilizing effect of the chemistry-dynamics coupling, which leads to weaker meridional temperature gradients and thus to a weaker polar vortex. But although this generally underlines the importance of a proper stratospheric representation for climate sensitivity studies, it is *not* automatically equivalent to a stratospheric control of the troposphere [*Plumb and Semeniuk*, 2003]. Instead, emerging stratospheric anomalies could initially be induced by preceding tropospheric cir-

culation changes. Nevertheless, between our particular simulations we only changed the coupling of stratospheric chemistry and dynamics. Thus, independent from the question of stratospheric or tropospheric control, our results prove that also originally stratospheric signals can be transported to the troposphere.

Beside the dynamical tropo-stratospheric coupling of the mid- to high latitudes there seems to be another coupling mechanism in the tropics, which is linked to variations of the global radiation balance. Our results demonstrate that within COUP there is a significant shift of -0.5 to -1 K for the zonal mean tropospheric temperatures between the AO phases in low latitudes. Since this shift does not appear without interactive chemistry (REF), it can be attributed to differing tropospheric impacts of lower stratospheric ozone. For COUP we showed that the ozone concentration in the tropical lower stratosphere enhances under AO+ conditions, and we also detected an increment in the zonal mean temperature for AO+, just above the tropical cooling. Obviously the enhanced AO+ ozone together with the high tropical insolation causes an additional radiative heating (which is not included in REF), leading to the increased lower stratospheric temperatures. At the same time this means an appropriate energy loss of the incoming solar radiation below, within the tropical troposphere, which produces the cooling there.

Thus, we detected a striking tropospheric tropical temperature response to stratospheric ozone changes, linked to the phase of the tropospheric mid- to highlatitudinal AO mode. Together with the shown sensitivity of the AO phase and the associated tropospheric planetary and synoptic scale wave activity to the interactive stratospheric ozone chemistry this clearly underlines the need to further detailed analyzes in this direction.

Acknowledgments.

We wish to thank U. Cubasch and I. Kirchner from FU Berlin (ECHO-G), MPI for Chemistry Mainz (MECCA), and R. Ruhnke and M. Wiehle from FZ Karlsruhe (chemistry boundary conditions) for providing model components or necessary data. We are grateful to K. Ketelsen for programming the coupling routines, and to S. Erxleben for programming support and preparing the graphics. K.D. and S.B. benefited from participating in the Virtual Institute "Pole-Equator-Pole" kept by the German Helmholtz Association.

References

Baldwin, M. P. and Dunkerton, T. J. (1999). Propagation of the Arctic Oscillation from the stratosphere to the troposphere. *J. Geophys. Res.*, 104:30937–30946.

Eichelberger, S. J. and Hartmann, D. L. (2005). Changes in the strength of the Brewer-Dobson circulation in a simple AGCM. *Geophys. Res. Lett.*, 32:15807–+.

Holton, J. R., Haynes, P. H., McIntyre, M. E., Douglass, A. R., Rood, R. B., and Pfister, L. (1995). Stratosphere-troposphere exchange. *Rev. Geophys.*, 33:403–440.

Huebener, H., Cubasch, U., Langematz, U., Spangehl, T., Niehörster, F., Fast, I., and Kunze, M. (2007). Ensemble climate simulations using a fully coupled ocean-troposphere-stratosphere general circulation model. *Phil. Trans. R. Soc. A*, 365:2089–2101.

Hurrell, J. W. (1995). Decadal Trends in the North Atlantic Oscillation: Regional Temperatures and Precipitation. *Science*, 269:676–679.

Kouker, W., Langbein, I., Reddmann, Th., and Ruhnke, R. (1999). The Karlsruhe Simulation Model of the Middle Atmosphere (KASIMA), Version 2. *Wiss. Berichte, FZKA*

6278, FZ Karlsruhe, Germany.

Legutke, S. and Voss, R. (1999). The Hamburg Atmosphere-Ocean Coupled Circulation Model ECHO-G. *Technical Report No. 18*, ISSN 0940-9327, DKRZ Hamburg, Germany.

Manzini, E. and McFarlane, N. A. (1998). The effect of varying the source spectrum of a gravity wave parameterization in a middle atmosphere general circulation model. *J. Geophys. Res.*, 103:31523–31540.

Morcrette, J. J. (1991). Radiation and cloud radiative properties in the European Center for Medium Range Weather Forecasts forecasting system. *J. Geophys. Res.*, 96:9121–9132.

Norton, W. A. (2003). Sensitivity of Northern Hemisphere surface climate to simulation of the stratospheric polar vortex. *Geophys. Res. Lett.*, 30:1627–+.

Plumb, R. A. and Semeniuk, K. (2003). Downward migration of extratropical zonal wind anomalies. *J. Geophys. Res.*, 108:4223–+.

Polvani, L. M. and Kushner, P. J. (2002). Tropospheric response to stratospheric perturbations in a relatively simple general circulation model. *Geophys. Res. Lett.*, 29:1114–+.

Rasch, P. J. and Williamson, D. L. (1990). On shape-preserving interpolation and semi-Lagrangian transport. *SIAM J. Sci. Stat. Comput.*, 11:656–687.

Roeckner, E., Arpe, K., Bengtsson, L., Christoph, M., Claussen, M., Dümenil, L., Esch, M., Giorgetta, M. A., Schlese, U., and Schulzweida, U. (1996). The atmospheric general circulation model ECHAM4: Model description and simulation of present-day climate. *Report No. 218*, MPI for Met. Hamburg, Germany.

Sander, R., Kerkweg, A., Jöckel, P., and Lelieveld, J. (2005). Technical note: The new

comprehensive atmospheric chemistry module MECCA. *Atmos. Chem. Phys.*, 5:445–450.

Scaife, A. A., Knight, J. R., Vallis, G. K., and Folland, C. K. (2005). A stratospheric influence on the winter NAO and North Atlantic surface climate. *Geophys. Res. Lett.*, 32:L18715.

Shindell, D. T., Schmidt, G. A., Miller, R. L., Rind, D. (2001). Northern Hemisphere winter climate response to greenhouse gas, ozone, solar, and volcanic forcing. *J. Geophys. Res.*, 106:7193–7210.

Song, Y. and Robinson, W. A. (2004). Dynamical mechanisms for stratospheric influences on the troposphere. *J. Atmos. Sci.*, 61:1711–1725.

Stenchikov, G., Robock, A., Ramaswamy, V., Schwarzkopf, M. D., Hamilton, K., Ramachandran, S. (2002). Arctic Oscillation response to the 1991 Mount Pinatubo eruption: Effects of volcanic aerosols and ozone depletion. *J. Geophys. Res. (Atm.)*, 107(D24):4803.

Thompson, D. W. J. and Wallace, J. M. (1998). The Arctic Oscillation signature in the wintertime geopotential height and temperature fields. *Geophys. Res. Lett.*, 25:1297–1300.

Torrence, C. and Compo, G. P. (1998). A practical guide to wavelet analysis. *Bull. Amer. Meteor. Soc.*, 79:61–78.

Wolff, J. O., Maier-Reimer, E., and Legutke, S. (1997). The Hamburg Ocean Primitive Equation Model HOPE. *Technical Report No. 13*, ISSN 0940-9327, DKRZ Hamburg, Germany.

Figure Captions

Figure 1 - DJF; model years 31 to 150: a) - Averaged z_{500}-differences in [gpm] between COUP and REF. The thick black contours mark 95% confidence areas for a Student's t-test based on yearly data. b) - DFT of the northern hemisphere z_{500}-fields: Logarithm of wave energy ($log(amp^2)$), (COUP-REF)/REF in [%]. Blue - mean of lowpass (10-90 d) filtered wavenumbers (WVN) 1-3, Red - mean of bandpass (2-6 d) filtered WVN's 4-10 (Blackmon filter). The shaded areas show the 1σ-uncertainties based on yearly data.

Figure 2 - DJF; model years 31 to 150: a) - PCA: PC1 of the z_{500}-field for COUP. PC1 is associated to the first Empirical Orthogonal Function (EOF1), giving the time evolution of this spatial pattern. Additionally shown are the selected 8-year periods representing the AO phases which were used to create the Figures 3a-c. b) - Local wavelet power spectrum of PC1, obtained with the Morlet wavelet. At both ends, dash-dotted lines separate regions where edge effects become important. The thick black contour envelopes areas exceeding the 95% confidence level for a corresponding red noise process.

Figure 3 - Zonal mean differences between the selected 8 model years representing the positive and 8 model years representing the negative phase of the Arctic Oscillation (AO). Also see figure 2a. a) - zonal wind u in [m/s]. b) - temperature T in [K]. c) - ozone concentration O_3 in $[10^{15}/m^3]$. The white lines show the confidence levels for Student's t-tests based on monthly data.

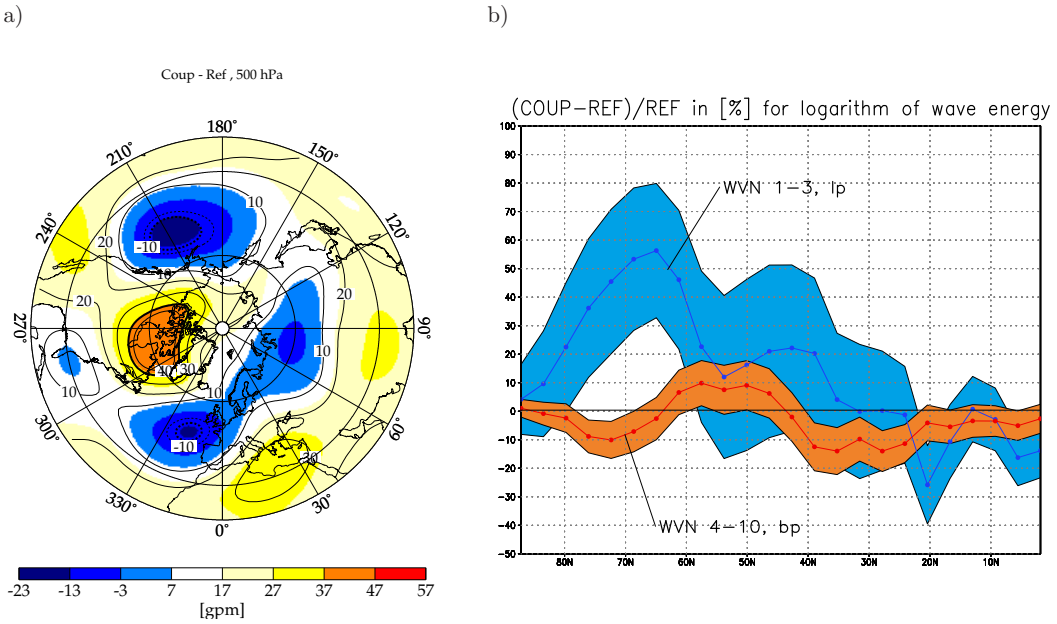

Figure 1.

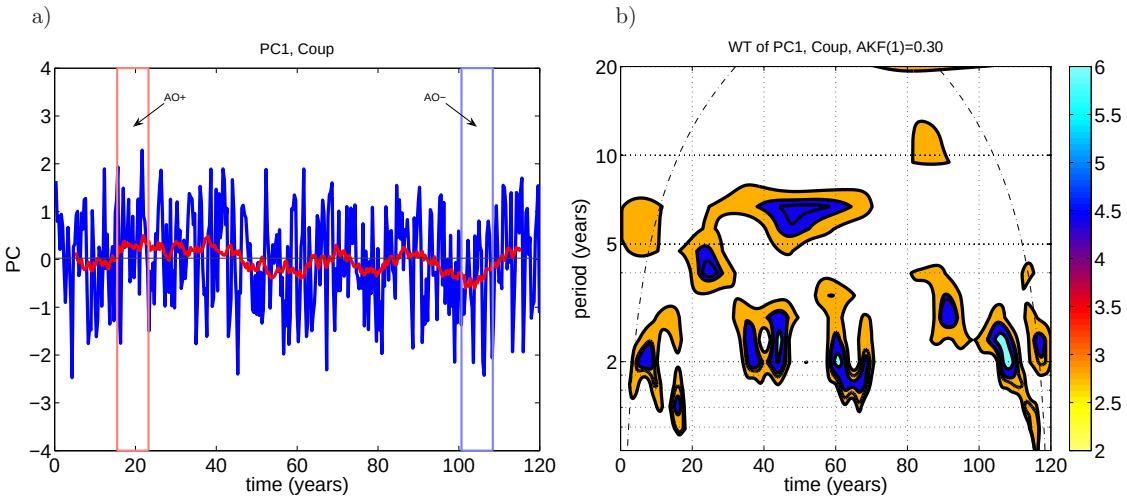

Figure 2.

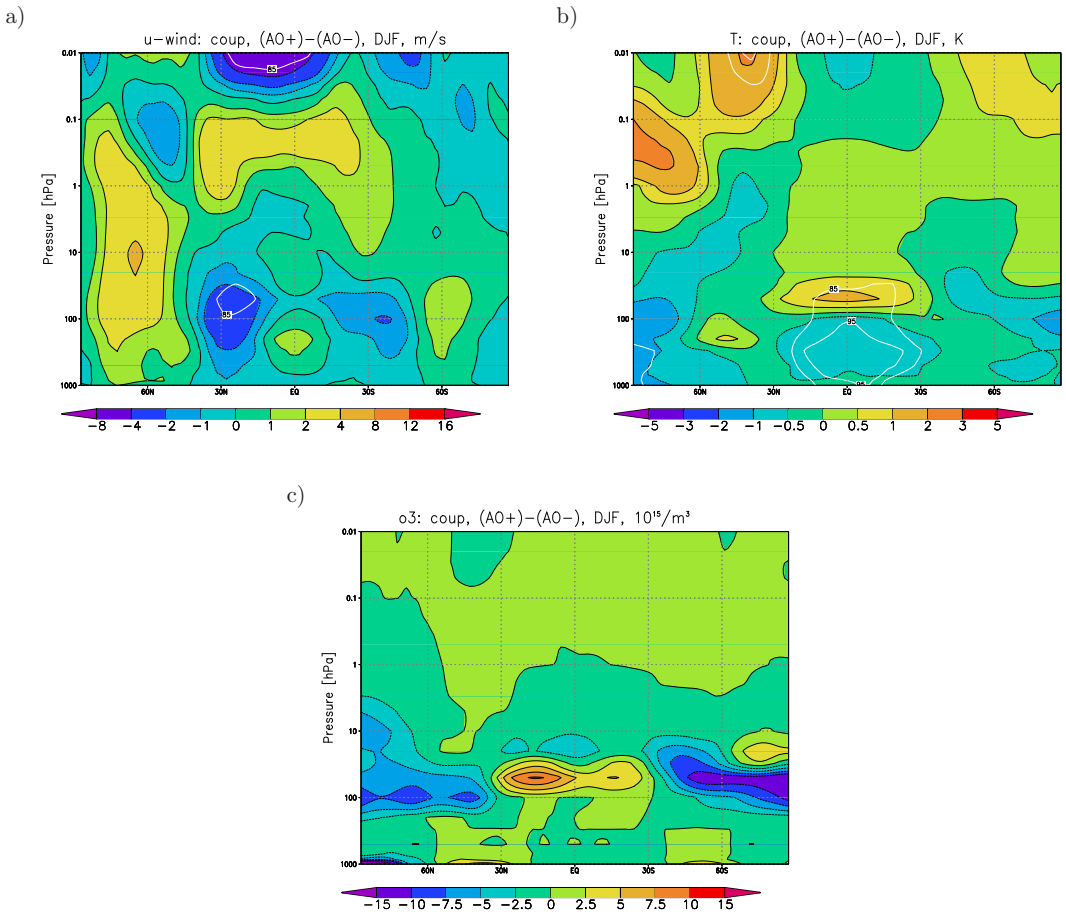
a)
u−wind: coup, (AO+)−(AO−), DJF, m/s
Pressure [hPa]
0.01
0.1
1
10
100
1000
60N
30N
EQ
30S
60S
−8 −4 −2 −1 0 1 2 4 8 12 16
b)
T: coup, (AO+)−(AO−), DJF, K
Pressure [hPa]
−5 −3 −2 −1 −0.5 0 0.5 1 2 3 5
c)
o3: coup, (AO+)−(AO−), DJF, 10¹⁵/m³
Pressure [hPa]
−15 −10 −7.5 −5 −2.5 0 2.5 5 7.5 10 15

Figure 3.